

Spatial Distribution of the Mean Peak Age of Information in Wireless Networks

Praful D. Mankar, Mohamed A. Abd-Elmagid, and Harpreet S. Dhillon

Abstract

This paper considers a large-scale wireless network consisting of source-destination (SD) pairs, where the sources send time-sensitive information, termed *status updates*, to their corresponding destinations in a time-slotted fashion. We employ Age of information (AoI) for quantifying the freshness of the status updates measured at the destination nodes for two different queuing disciplines, *namely* Type I and II queues. Type I queue is assumed to transmit the status updates in a first-come-first-served (FCFS) fashion with no storage facility. However, Type I queue may not necessarily minimize AoI because a new update will not be allowed to enter a server until the current update has been successfully transmitted. To overcome this shortcoming, we consider Type II queue in which the most recent status update available at a given transmission slot is transmitted in order to minimize the AoI. As the update delivery rate for a given link is a function of the interference field seen from the receiver, the temporal mean AoI can be treated as a random variable over space. Our goal in this paper is to characterize the spatial distribution of the mean AoI observed by the SD pairs by modeling them as a Poisson bipolar process. Towards this objective, we first derive accurate bounds on the moments of success probability while efficiently capturing the interference-induced coupling in the activities of the SD pairs. Using this result, we then derive tight bounds on the moments as well as the spatial distribution of peak AoI. Our numerical results verify our analytical findings and demonstrate the impact of various system design parameters on the mean peak AoI.

Index Terms

Age of information, bipolar Poisson point process, stochastic geometry, and wireless networks.

The authors are with Wireless@VT, Bradley Department of Electrical and Computer Engineering, Virginia Tech, Blacksburg, VA. Email: {prafuldm, maelaziz, hdhillon}@vt.edu. The support of the U.S. NSF (Grant CPS-1739642) is gratefully acknowledged. This paper is submitted in part to IEEE Globecom 2020 [1].

I. INTRODUCTION

With the emergence of Internet of Things (IoT), wireless networks are expected to provide a reliable platform for enabling real-time monitoring and control applications. Many such applications, such as the ones related to air pollution or soil moisture monitoring, involve a large-scale deployment of IoT sensors, which would acquire updates about some underlying random process and send them to the destination nodes (or monitoring stations). Naturally, accurate quantification of the freshness of status updates received at the destination nodes is essential in such applications. However, the traditional performance metrics of communication systems, like throughput and delay, are not suitable for this purpose since they do not account for the generation times of status updates. This has recently motivated the use of AoI to quantify the performance of communication systems dealing with the transmission of time-sensitive information [2]. This metric was first conceived in [3] for a simple queuing-theoretic model in which randomly generated update packets arrive at a source node according to a Poisson process, and then transmitted to a destination node using a first-come-first-served (FCFS) queuing discipline. In particular, AoI was defined in [3] as the time elapsed since the latest successfully received update packet at the destination node was generated at the source node. As evident from the definition, AoI is capable of quantifying how *fresh* the status updates are when they reach the destination node since it tracks the generation time of each update packet. As will be discussed next in detail, the analysis of AoI has mostly been limited to simple settings that ignore essential aspects of wireless networks, including temporal channel variations and random spatial distribution of nodes. This paper presents a novel spatio-temporal analysis of AoI in a wireless network by incorporating the effect of both the channel variations and the randomness in the wireless node locations to derive the spatial distribution of the temporal mean AoI.

A. Prior Art

For a point-to-point communication system, the authors of [3] characterized a closed-form expression for the average AoI. Using this result, they demonstrated that the optimal rate at which the source should generate its update packets in order to minimize the average AoI is different from the optimal rates that either maximize throughput or minimize delay. Subsequently, the authors of [4]–[11] characterized the average AoI or similar age-related metrics (e.g., peak AoI [5], [8], [9] and Value of Information of Update [10]) for a variety of the queuing disciplines. In

addition, the authors of [12]–[16] presented the queuing theory-based analysis of the distribution of AoI. The above works provide foundational understanding of temporal variations of AoI from the perspective of queuing theory for a point-to-point communication system. Inspired by these works, the AoI or similar age-related metrics have been used to characterize the performance of real-time monitoring services in a variety of communication systems, including broadcast networks [17]–[19], multicast networks [20], [21], multi-hop networks [22], [23], multi-server information-update systems [24], IoT networks [25]–[30], cooperative device-to-device (D2D) communication networks [31], [32], unmanned aerial vehicle (UAV)-assisted networks [33], [34], ultra-reliable low-latency vehicular networks [35], and social networks [36]–[38]. All these studies mostly focus on minimizing the AoI with the following design objectives: 1) design of scheduling policies [17]–[19], [22], [30], 2) design of cooperative transmission policies [20]–[23], [31], [32], 3) design of the status update sampling policies [27]–[29], [36], and 4) trade-off with other performances metrics in heterogeneous traffic/networks scenarios [23]–[25], [29], [37]. However, given the underlying tools used, these works are not conducive to account for some important aspects of wireless networks, such as interference, channel variations, path-loss, and randomness in the wireless network topologies. Specifically, it is not possible to capture interference-induced stochastic interactions among the wireless nodes using the tools developed in the above works that either rely on a standalone application of queuing theory or focus on the AoI-optimal update policies in simple network topologies. Hence, these analyses can not be directly extended to describe the spatial AoI performance disparity that is inherently present in the wireless networks as will be evident shortly.

In a wireless network, the AoI measured at a destination primarily depends on the ability of its source to successfully transmit status updates in the presence of interference from the simultaneous transmissions of the other sources. Specifically, the temporal mean AoI of a typical SD pair depends on its rate of successful transmission in the presence of interference. Therefore, the probability of successful transmission is a function of the spatial pattern of interfering sources as seen by the destination node, which has never been studied in the literature. This introduces the spatial disparity in the temporal mean AoI experienced by the SD pairs irregularly spread across the networks. In order to study this, we need a way to rigorously model spatial distributions of wireless nodes, which can be done using stochastic geometry. The tools from stochastic geometry has gained significant popularity in the recent past for the modeling and analysis of

a variety of wireless networks such as cellular networks [39], heterogeneous networks [40] and ad-hoc networks [41]. However, the analysis of traffic aware metrics, such as delay and AoI, using stochastic geometry-based models is known to be hard because of the interference-induced coupling in the transmission activities of the wireless nodes. As a result, while there are a handful of recent works focusing on the application of stochastic geometry to AoI [42]–[45], their scope is limited to the analysis of the spatio-temporal mean of AoI ([42]) or the peak AoI ([43], [44]), which is not sufficient to describe the spatial disparity in AoI, as described above. Motivated by this, we develop a stochastic geometry-based analytical framework for accurately determining the spatial distribution of the mean peak AoI experienced by the wireless links spread across the network.

B. Contributions

This paper presents a stochastic geometry-based analysis of AoI for a large-scale wireless network, wherein the sources transmit time-sensitive status updates to their corresponding destinations. In particular, we derive the spatial distribution of mean peak AoI while assuming that the locations of SD pairs follow a homogeneous bipolar Poisson point process (PPP). In order to overcome the challenge of interference-induced coupling across queues associated with different SD pairs, we propose a tractable two-step analytical approach which relies on a careful construction of *dominant systems*. The proposed framework efficiently captures the stochastic interaction in both space (through interference) and time (through random transmission activities). Our approach provides a much tighter lower bound on the spatial moments of the conditional (location-dependent) successful transmission probability compared to the existing stochastic geometry-based analyses, e.g., [46], which mainly rely on the assumption of having saturated queues at the interfering nodes.

Further using the lower bounds of the moments of the success probability, we derive tighter upper bounds on the spatial moments of the temporal mean peak AoI for two different queue disciplines, *namely* Type I and Type II queues. We consider that status updates arriving at the sources follow independent but identical Bernoulli processes under both of these queues. Further, the sources are assumed to transmit status updates to their destinations in a FCFS manner without any storage facility (i.e., zero buffer) under Type I queue. The analysis of such a queue (with no storage facility) is meaningful since the storage of constantly ageing status updates may not

improve the AoI performance drastically, especially when the updates arrive frequently. However, Type I queue may not necessarily minimize AoI because a new update will not be allowed to enter a server until the current update has been successfully transmitted. Inspired by this, we consider the Type II queue, in which we assume that each source transmits the most recently available status update in a given time slot by simply discarding the current update in server, if any. This queue discipline is in fact optimal from the perspective of minimizing the AoI as it always transmits the most recent update available. To the best of the authors knowledge, this is the first attempt to characterize the spatial distribution of temporal mean peak AoI for the wireless networks. The contributions of this paper are briefly summarized as below.

- 1) This paper presents a novel analytical framework to determine close lower bounds on the moments of the conditional success probability while efficiently capturing the interference-induced coupling in the activities of SD pairs.
- 2) We derive the temporal mean of peak AoI under Type I and Type II queue disciplines for a given success probability of transmission.
- 3) Next, using the lower bounds on the moments of the conditional success probability, we derive tight upper bounds on the spatial moments of the temporal mean peak AoI for both Type I and II queues.
- 4) Using the beta approximation for the distribution of conditional success probability [47], we also characterize the spatial distribution of temporal mean peak AoI for both queuing disciplines.
- 5) Next, we validate the accuracy of the proposed analytical framework for AoI analysis through extensive simulations. Finally, our numerical results reveal the impact of key design parameters, such as the medium access probability, update arrival rate, and signal-to-interference (SIR) threshold, on the spatial mean and standard deviation of the temporal mean peak AoI observed under the aforementioned queuing disciplines.

II. SYSTEM MODEL

We model the source-destination pairs using a Poisson bipolar model wherein the locations of sources follow PPP Φ with density λ_{sd} and their corresponding destinations are located at fixed distance R from them in uniformly random directions. From Slivnyak's theorem, we know that conditioning on a point is the same as adding a point to a PPP [48]. Therefore, without

loss of generality, we perform the analysis for the typical link whose destination and source are placed at the origin and $\mathbf{x}_o \equiv [R, 0]$, respectively. Fig. 1 presents a representative realization of the Poisson bipolar network with the typical link placed at the origin.

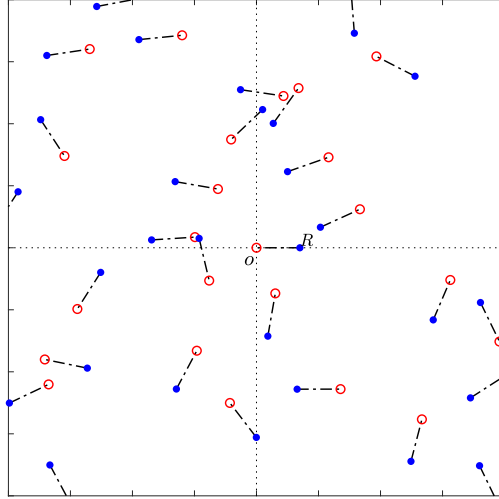


Figure 1. An illustration of the Poisson bipolar network. Blue dots and red circles represent the locations of sources and destinations, respectively.

The SIR measured at the typical destination in the k -th transmission slot is

$$\text{SIR}_k = \frac{h_{\mathbf{x}_o,k} R_o^{-\alpha}}{\sum_{\mathbf{x} \in \Phi} h_{\mathbf{x},k} \|\mathbf{x}\|^{-\alpha} \mathbf{1}(\mathbf{x} \in \Phi_k)}, \quad (1)$$

where Φ_k is the set of sources with active transmission during the k -th transmission slot, α is the path-loss exponent, and $h_{\mathbf{x},k}$ is the channel gain for the link between the source at \mathbf{x} and the typical destination at the origin in transmission slot k . We assume quasi-static Rayleigh fading and model, which implies $h_{\mathbf{x},k} \sim \exp(1)$ independently across both $\mathbf{x} \in \Phi$ and $k \in \mathbb{N}$.

A. Conditional Success Probability

The transmission is considered to be successful when the received SIR is greater than a threshold β . From (1), it is clear that the successful transmission probability measured at the typical destination placed at o depends on the PPP Φ of the interfering sources and is given by

$$\begin{aligned} \mu_{\Phi} &= \mathbb{P}[\text{SIR}_k > \beta | \Phi], \\ &= \mathbb{P} \left[h_{\mathbf{x}_o,k} > \beta R^{\alpha} \sum_{\mathbf{x} \in \Phi} h_{\mathbf{x},k} \|\mathbf{x}\|^{-\alpha} \mathbf{1}(\mathbf{x} \in \Phi_k) \right], \end{aligned}$$

$$\begin{aligned}
&= \exp \left(\beta R^\alpha \sum_{\mathbf{x} \in \Phi} h_{\mathbf{x},k} \|\mathbf{x}\|^{-\alpha} \mathbf{1}(\mathbf{x} \in \Phi_k) \right), \\
&= \prod_{\mathbf{x} \in \Phi} \frac{p_{\mathbf{x}}}{1 + \beta R^\alpha \|\mathbf{x}\|^{-\alpha}} + (1 - p_{\mathbf{x}}),
\end{aligned} \tag{2}$$

where $p_{\mathbf{x}}$ represents the probability that the source at $\mathbf{x} \in \Phi$ is active. The above conditional success probability μ_{Φ} directly governs packet delivery rate at the typical destination for a given Φ . Therefore, knowledge of the distribution of the conditional success probability, termed *meta distribution* [47], is crucial to characterize the queue performance for the typical SD pair.

B. Traffic Model and AoI Metric

We consider that sources transmit updates to their corresponding destinations regarding some random processes $H(t)$ s. It is assumed that the updates of these random processes arrive at the sources independently according to a Bernoulli process with parameter λ_a . The successful delivery of an update takes a random number of transmissions depending on the channel conditions that further depend on numerous factors, such as fading coefficients, received interference power, and network congestion. Links that are in close proximity of each other may experience arbitrarily small update delivery rate because of severe interference, especially when update arrival rate is high. Therefore, to alleviate the impact of severe interference in such cases, we assume that each source attempts transmission with probability ξ independently of the other sources in a given time slot. Also note that the probability of the attempted transmission being successful in a given time slot is the conditional success probability μ_{Φ} because of the assumption of independent fading. Therefore, the number of slots needed for delivering an update at the typical destination can be modeled using the geometric distribution with parameter $\xi \mu_{\Phi}$ for a given Φ .

Our aim is to characterize the AoI of the random process $H(t)$ at the typical destination, where $H(t)$ is the random process observed by the typical source. Let t_k and t'_k be the time instances of the arrival and reception of the k -th update at the source and destination, respectively. Given time s , let $N(s) = \max\{k | t'_k \leq s\}$ be the instant of the most recently received update and $U(s) = t_{N(s)}$ be the time stamp of the generation of the most recently received update. The AoI is defined as the random process

$$\Delta(t) = t - U(t). \tag{3}$$

The AoI $\Delta(t)$ increases linearly with time and drops upon reception of a new update at the destination to the total time experienced by this new update in the system. Note that the

minimum possible AoI is one because we assume arrival and delivery of an update to occur at the beginning and the end of the transmission slots, respectively. Note that $T_k = t'_k - t_k$ is the time spent by the k -th update in the system and $Y_k = t'_k - t'_{k-1}$ is the time elapsed between the receptions of the $(k-1)$ -th and k -th updates. Given this background, we are now ready to define peak AoI, which will be studied in detail in this paper.

Definition 1 (Peak AoI). *The peak AoI is defined in [5] as the value of AoI process $\Delta(t)$ measured immediately before the reception of the k -th update and is given by*

$$A_k = T_{k-1} + Y_k. \quad (4)$$

As evident from the above discussion, the mean peak AoI measured at the typical destination depends on the conditional success probability μ_Φ and hence the mean peak AoI is a random variable. Therefore, our goal is to determine the distribution of the conditional mean peak AoI of the SD pairs distributed across the network. In the following we define the distribution of mean peak AoI.

Definition 2. *The complementary cumulative distribution function (CDF) of the conditional mean peak AoI is defined as*

$$\bar{F}(x; \beta) = \mathbb{P}[\bar{A}(\beta; \Phi) > x], \quad (5)$$

where $\bar{A}(\beta; \Phi) = \mathbb{E}[A_k | \beta; \Phi]$ is the conditional mean peak AoI measured at the typical destination for given Φ and SIR threshold β .

C. Queue Disciplines

This paper considers two types of queue disciplines which are referred to as Type I and Type II queues. For the Type I queue, we assume that the updates are transmitted based on a first-come-first-serve (FCFS) basis with no storage facility (i.e., zero buffer). This queuing discipline is meaningful because it drops updates that cannot be transmitted when the server is busy, thereby allowing fresh update to be accommodated after the current transmission is successful. The only disadvantage of this scheme is that if the server takes a long time to transmit the packet (because of failed transmission attempts), the update in the server gets stale, which impacts AoI at the destination. Inspired by this, we consider the Type II queue wherein the current update gets replaced by the new update whenever it arrives in the system. Because of this, the source always

ends up transmitting the most recent update whenever the transmission is successful. Therefore, Type II queue is in fact optimal from the perspective of minimizing AoI at the destination. That said, the analysis of Type I queue is still important because it acts as the precursor for the more complicated analysis of Type II queue.

We first present the analysis of the conditional mean peak AoI $\bar{A}(\beta; \Phi)$ for the Type I queue discipline in Section III. Next, we extend the analysis for the Type II queue discipline in Section IV using the analytical framework developed in Section III.

III. AOI FOR THE TYPE I QUEUE

The Type I queue transmits updates according to the FCFS policy without buffering the randomly arriving status updates. As a result, the updates arriving during the ongoing transmission (i.e., busy server) are dropped. The sample path of the AoI process for the Type I queue is illustrated in Fig. 2. The red upward and blue downward arrow marks indicate the

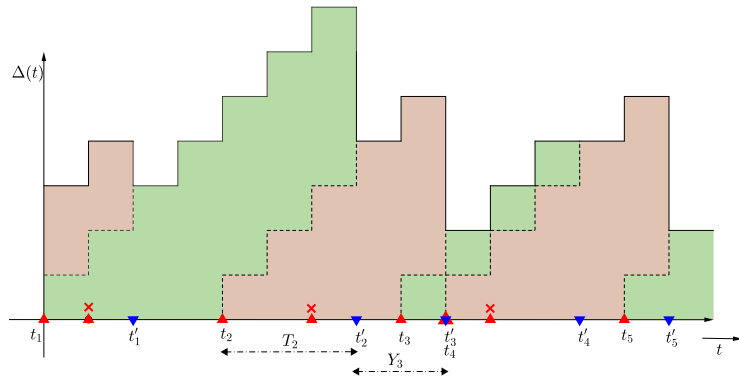


Figure 2. Sample path of the AoI $\Delta(t)$ under the Type I queue discipline.

arrival and reception of updates at the source and destination, respectively. The red cross marks indicate the instances of dropped updates which arrive while the server is busy. We first derive the conditional mean peak AoI $\bar{A}(\beta; \Phi)$ for Type I queue in the following subsection. In the subsequent subsections, we will develop an approach to derive the distribution of $\bar{A}(\beta; \Phi)$ using stochastic geometry.

A. Conditional Mean Peak AoI

As discussed in Section II-B, the update delivery rate is governed by the product of the medium access probability ξ and the conditional success probability μ_Φ . Thus, for a given Φ ,

the mean number of slots required for successful transmission of an update is

$$\mathbb{E}[T_k] = \frac{1}{\mu_\Phi \xi}.$$

Since we assumed zero length buffer queue, the next transmission is possible only for the update arriving after the successful reception of the ongoing update. Therefore, the time between the successful reception of $(k-1)$ -th and k -th updates is

$$Y_k = S_k + T_k,$$

where S_k is the number of slots required for the k -th update to arrive after the successful delivery of the $(k-1)$ -th update. Since the transmission of the next new update (after successful delivery) begins in the same slot in which it arrives, we have $S_k \in \{0, 1, \dots\}$. Thus, the pmf of S_k can be modeled using a geometric distribution with parameter $\lambda'_a = \lambda_a / (1 - \lambda_a)$. Therefore, we get

$$\mathbb{E}[S_k] = \frac{1}{\lambda'_a}.$$

Now, from (4), the conditional mean peak AoI for given Φ becomes

$$\bar{A}_1(\beta; \Phi) = \mathcal{Z}_a + \frac{2}{\mu_\Phi \xi}, \quad (6)$$

where $\mathcal{Z}_a = \frac{1}{\lambda'_a}$. Using (6) and the distribution of μ_Φ , we can directly determine the distribution of $\bar{A}_1(\beta; \Phi)$. However, from (2), it can be seen that the knowledge of probability p_x of the interfering source at $x \in \Phi$ being active is required to determine the distribution of μ_Φ . For this purpose, we first determine the activity of the typical source for a given μ_Φ in the following subsection which will later be used to define the activities of interfering sources in order to characterize the distribution of μ_Φ .

B. Conditional Activity

As we assume that each source attempts transmission independently in a given time slot with probability ξ , the conditional probability of the typical source having an active transmission becomes

$$\zeta_o = \xi \pi_1, \quad (7)$$

where π_1 is the conditional steady state probability that the source has an update to transmit. Thus, ζ_o depends on the probability p_x of the interfering source at $x \in \Phi$ being active through the conditional success probability μ_Φ (see (2)).

The steady state distribution of a queue is characterized by its arrival and departure processes.

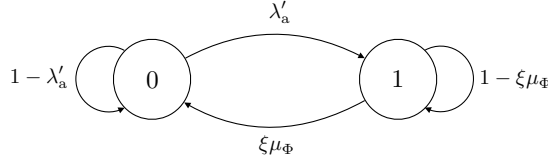


Figure 3. State Diagram of the Type I queue. States 0 and 1 respectively signify idle and busy states of the typical source.

In our case, both the arrivals and departures of the updates of $H(t)$ follow geometric distributions with parameters λ'_a and $\xi\mu_\Phi$, respectively. Fig. 3 shows the state diagram for the Type I queue. The steady state distribution can be directly determined as

$$\pi_0 = \frac{\xi\mu_\Phi}{\lambda'_a + \xi\mu_\Phi} \quad \text{and} \quad \pi_1 = \frac{\lambda'_a}{\lambda'_a + \xi\mu_\Phi} \quad (8)$$

where π_0 and π_1 are the probabilities of states 0 and 1, respectively.

C. Meta Distribution

From the above it is clear that the mean peak AoI jointly depends on the PPP Φ of the interfering sources and their activities p_x through the conditional success probability μ_Φ . Hence, the knowledge of the exact distribution of μ_Φ , i.e., $\mathbb{P}[\mu_\Phi \leq x]$, is essential for characterizing the spatial distribution of the mean peak AoI. However, it is very challenging to capture the temporal correlation among the activities of the sources in the success probability analysis. Therefore, we present the moments and approximate distribution of μ_Φ in the following lemma while assuming the activities p_x to be independent and identically distributed (i.i.d.).

Lemma 1. *The b -th moment of the conditional success probability μ_Φ is*

$$M_b = \exp \left(-\pi \lambda_{sd} \beta^\delta R^2 \hat{\delta} C_{\zeta_o}(b) \right), \quad (9)$$

where $\delta = \frac{2}{\alpha}$, $\hat{\delta} = \Gamma(1 + \delta)\Gamma(1 - \delta)$ and

$$C_{\zeta_o}(b) = \sum_{m=1}^{\infty} \binom{b}{m} \binom{\delta - 1}{m - 1} \bar{p}_m,$$

and \bar{p}_m is the m -th moment of the activity probability. The meta distribution can be approximated with the beta distribution as

$$\mathbb{P}[\mu_\Phi \leq x] \approx I_x(\kappa_1, \kappa_2), \quad (10)$$

where $I_x(\cdot, \cdot)$ is the regularized incomplete beta function and

$$\kappa_1 = \frac{M_1 \kappa_2}{1 - M_1} \quad \text{and} \quad \kappa_2 = \frac{(M_1 - M_2)(1 - M_1)}{M_2 - M_1^2}. \quad (11)$$

Proof. Refer to Appendix A for the proof of moments of μ_Φ . \square

It must be noted that the distribution of the conditional success probability μ_Φ is approximated using the beta distribution by equating the first two moments, similar to [47]. Now, we present an approach for accurate characterization of μ_Φ in the following subsection.

D. Analysis under Correlated Queues

As discussed in Section III-B, the activity of the typical source depends on its successful transmission probability which further depends on the activities of the other sources in Φ through interference (refer to (2)). Besides, the transmission of the typical source causes strong interference to its neighbouring sources which in turn affects their activities. Hence, the successful transmission probabilities of the typical source and its neighbouring sources are correlated through interference which introduces coupling between the operations of their associated queues. As the exact analysis of the correlated queues is complex, the usual practice for analyzing such systems is to make meaningful modifications (refer to [49]) so that useful bounds on the network performance can be derived. The readers can refer to [46], [50], [51] for a small subset of relevant works in the context of wireless networks.

For a modified system, the general approach, called as *dominant system*, considers the full buffer assumption for the interfering links to remove correlation in their transmission [49]. The authors of [50] employed the second degree of modification to the system for further improving the performance bound obtained through the dominant system. For this second degree of modification, the authors assume that the interfering nodes operate at their minimum service rates obtained through their corresponding dominant systems. Refer to [50] for more details on this. Naturally, the second level modification will provide a better lower bound on the success probability as it estimates the interference (for a given traffic load) more accurately as compared to the dominant system. On the similar lines of [50], we present a novel two-steps analytical framework to enable an accurate success probability analysis using stochastic geometry while accounting for the temporal correlation in the queues associated with the SD pairs.

- Step 1 (*Dominant System*): For the dominant system, the interfering sources having no updates to transmit are assumed to transmit dummy packets with probability ξ . As a result, the success probability measured at the typical destination is a lower bound to that in the

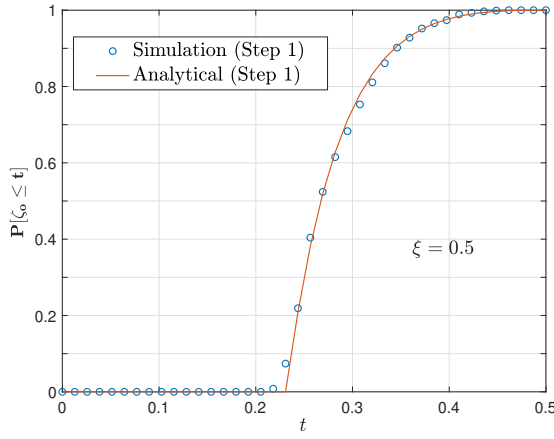


Figure 4. Verification of the CDF of the activity in the dominant system.

original system. The b -th moment and approximate distribution of μ_Φ for the dominant system can be evaluated using Lemma 1 by setting $\bar{p}_m = \xi^m$. Using (7), we can obtain the distribution of the activity of the typical source in the dominant system as

$$\mathbb{P}[\zeta_o \leq t] = \mathbb{P}\left[\lambda'_a \left(\frac{1}{t} - \frac{1}{\xi}\right) \leq \mu_\Phi\right] \approx 1 - I_{\lambda'_a(\frac{1}{t} - \frac{1}{\xi})}(\kappa_1, \kappa_2), \quad (12)$$

for $0 < t \leq \xi$, where κ_1 and κ_2 are evaluated using (11) by setting $\bar{p}_m = \xi^m$. It is quite evident that the activity ζ_o is less than ξ which is also consistent with the assumption of setting $p_x = \xi$ for $\forall x \in \Phi$ to define the dominant system. Fig. 4 illustrates the accuracy of the above approximate distribution of the activity of the typical source under the dominant system. Using (12), the m -th moment of the activity of the typical source in this dominant system can be evaluated as

$$\bar{p}_m^D = m \int_0^\xi t^{m-1} \mathbb{P}[\zeta_o > t] dt = m \int_0^\xi t^{m-1} I_{\lambda'_a(\frac{1}{t} - \frac{1}{\xi})}(\kappa_1, \kappa_2) dt, \quad (13)$$

where the κ_1 and κ_2 are evaluated using (11) by setting $\bar{p}_m = \xi^m$.

- **Step 2 (Second-Degree of System Modifications):** Inspired by [50], we construct a second-degree system in which each interfering source is assumed to operate in the dominant system described in Step 1 (i.e., the interference field seen by a given interfering source is constructed based on Step 1). The typical SD link is now assumed to operate under these interfering courses. Naturally, the activities of the interfering sources will be higher in this modified system compared to those in the original system. As a result, the typical SD link will experience increased interference, and hence its conditional success probability will be a lower bound to that in the original system. It is easy to see that activities of the sources

(in their dominant systems) are identically but not independently distributed. However, as is standard in similar stochastic geometry-based investigations, we will assume them to be independent to make the analysis tractable. In other words, we model the activities of the interfering sources in this modified system independently using the activity distribution presented in (12) for the typical SD link in its dominant system. As demonstrated in Section V, this assumption does not impact the accuracy of our results. Hence, similar to Step 1, the b -th moment and the approximate distribution of μ_Φ for this second-degree modified system can be determined using Lemma 1 by setting $\bar{p}_m = \bar{p}_m^D$.

E. Moments and Distribution of $\bar{A}_1(\beta; \Phi)$

Here, we derive the bounds on the moments and distribution of the conditional mean peak AoI $\bar{A}_1(\beta; \Phi)$ using the two-step analysis of conditional success probability presented in Sections III-C and III-D.

Theorem 1. *The upper bound of the b -th moment of the conditional mean peak AoI for Type I queue is*

$$Q_b = \sum_{n=0}^b \binom{b}{n} \mathcal{Z}_a^{b-n} 2^n \xi^{-n} \exp\left(-\pi \lambda_{sd} \beta^\delta R^2 \hat{\delta} C_{\zeta_o}(-n)\right), \quad (14)$$

where

$$C_{\zeta_o}(-n) = \sum_{m=1}^{\infty} \binom{-n}{m} \binom{\delta-1}{m-1} \bar{p}_m^D,$$

and \bar{p}_m^D is given in (13).

Proof. Using (6), the b -th moment of the conditional mean peak AoI can be determined as

$$Q_b = \mathbb{E}_\Phi \left[(2(\xi \mu_\Phi)^{-1} + \mathcal{Z}_a)^b \right] \stackrel{(a)}{=} \sum_{n=0}^b \binom{b}{n} \mathcal{Z}_a^{b-n} 2^n \xi^{-n} M_{-n} \quad (15)$$

where (a) follows using the binomial expansion and $\mathbb{E}[\mu_\Phi^{-n}] = M_{-n}$. According to the Step 2 discussed in Subsection III-D, M_{-n} can be obtained using Lemma 1 by setting $\bar{p}_m = \bar{p}_m^D$. Recall that the two-step analysis provides a lower bound on the success probability μ_Φ because of overestimating the activities of the interfering sources. Therefore, the b -th moment of $\bar{A}_1(\beta; \Phi)$ given in (14) is indeed an upper bound since $\bar{A}_1(\beta; \Phi)$ is inversely proportional to μ_Φ . \square

In the following corollary, we present the simplified expressions for the evaluation of the first two moments of $\bar{A}_1(\beta; \Phi)$.

Corollary 1. *The upper bound of the first two moments of the conditional mean peak AoI for Type I queue are*

$$Q_1 = \mathcal{Z}_a + 2\xi^{-1}M_{-1} \quad (16)$$

$$Q_2 = \mathcal{Z}_a^2 + 4\mathcal{Z}_a\xi^{-1}M_{-1} + 4\xi^{-2}M_{-2} \quad (17)$$

and the upper bound of its variance is

$$\text{Var} = 4\xi^{-2} (M_{-2} - M_{-1}^2), \quad (18)$$

where $M_l = \exp\left(-\pi\lambda_{sd}\beta^\delta R^2 \hat{\delta} C_{\zeta_o}(l)\right)$ and

$$C_{\zeta_o}(-1) = -\mathbb{E} [\zeta_o(1 - \zeta_o)^{\delta-1}]$$

$$\text{and } C_{\zeta_o}(-2) = (\delta - 1)\mathbb{E} [\zeta_o(1 - \zeta_o)^{\delta-2}] - (\delta + 1)\mathbb{E} [\zeta_o(1 - \zeta_o)^{\delta-1}],$$

and distribution of ζ_o is given in (12).

Proof. Solving (15) for $b = \{1, 2\}$ and then substituting M_{-1} and M_{-2} from Lemma 1, we obtain (16)-(18). From the definition of $C_{\zeta_o}(b)$, we can directly determine

$$C_{\zeta_o}(-1) = \mathbb{E} \left[\sum_{m=1}^{\infty} \binom{-1}{m} \binom{\delta-1}{m-1} \zeta_o^m \right] = -\mathbb{E} [\zeta_o(1 - \zeta_o)^{\delta-1}].$$

Now, for $b = -2$, let $C_{\zeta_o}(-2) = \mathbb{E}[B(\zeta_o, -2)]$ where

$$\begin{aligned} B(\zeta_o, -2) &= \sum_{m=1}^{\infty} \binom{-2}{m} \binom{\delta-1}{m-1} \zeta_o^m, \\ &= \sum_{m=1}^{\infty} (-1)^{2m-1} (m+1) \binom{m-1-\delta}{m-1} \zeta_o^m, \\ &= -\sum_{m=1}^{\infty} (m-\delta) \frac{\Gamma(m-\delta)}{\Gamma(1-\delta)\Gamma(m)} \zeta_o^m + (\delta+1) \binom{m-1-\delta}{m-1} \zeta_o^m, \\ &= -\sum_{m=1}^{\infty} \frac{\Gamma(2-\delta)}{\Gamma(2-\delta)} \frac{\Gamma(m-\delta+1)}{\Gamma(1-\delta)\Gamma(m)} \zeta_o^m + (\delta+1) \binom{m-1-\delta}{m-1} \zeta_o^m, \\ &= -\sum_{m=1}^{\infty} \frac{\Gamma(2-\delta)}{\Gamma(1-\delta)} \binom{m-\delta}{m-1} \zeta_o^m + (\delta+1) \binom{m-1-\delta}{m-1} \zeta_o^m, \\ &= -(1-\delta) \sum_{m=1}^{\infty} \binom{m-\delta}{m-1} \zeta_o^m - (\delta+1) \sum_{m=1}^{\infty} \binom{m-1-\delta}{m-1} \zeta_o^m, \\ &= (\delta-1) \zeta_o \sum_{l=0}^{\infty} \binom{l+1-\delta}{l} \zeta_o^l - (\delta+1) \zeta_o \sum_{l=0}^{\infty} \binom{l-\delta}{l} \zeta_o^l \end{aligned}$$

$$= (\delta - 1)\zeta_o(1 - \zeta_o)^{\delta-2} - (\delta + 1)\zeta_o(1 - \zeta_o)^{\delta-1}.$$

Finally, taking expectation of $B(\zeta_o, -2)$ with respect to ζ_o provides $C_{\zeta_o}(-2)$. \square

Remark 1. For the mean peak AoI given in (16), the first term captures the impact of the update arrival rate λ_a whereas the second term depends on the inverse mean of the conditional success probability, which captures the impact of the wireless link parameters such as the link distance R , network density λ_{sd} , and path-loss exponent α . However, from (18), we can see that the variance of the mean peak AoI is independent of the arrival rate of updates and completely depends on the link quality parameters.

Now, using the beta approximation of the conditional success probability presented in Lemma 1, we determine the distribution of $\bar{A}_1(\beta; \Phi)$ in the following corollary.

Corollary 2. Under the beta approximation, the CDF of the conditional mean peak AoI for Type I queue is

$$F(x; \beta) = 1 - I_{2\xi^{-1}(x - \mathcal{Z}_a)^{-1}}(\kappa_1, \kappa_2), \quad (19)$$

where κ_1 and κ_2 are obtain using Lemma 1 by setting $\bar{p}_m = \bar{p}_m^D$.

Proof. Using (6) and the beta approximation of the distribution of μ_Φ given in Lemma 1, we can determine the distribution of $\bar{A}_1(\beta; \Phi)$ as

$$\mathbb{P}[\bar{A}_1(\beta; \Phi) \leq x] = \mathbb{P}[\mu_\Phi \geq 2\xi^{-1}(x - \mathcal{Z}_a)^{-1}].$$

Further, using the beta approximation for the distribution of μ_Φ (given in Lemma 1), we obtain (19). The parameters κ_1 and κ_2 need to be determined for $\bar{p}_m = \bar{p}_m^D$ (refer to Section III-D). \square

IV. AOI FOR TYPE II QUEUE

The Type II queue is assumed to transmit the most recent update available at the source in a given transmission slot. As implied by its definition, the Type II queue helps reduce the AoI which is clearly significant when the update arrival rate is high while the delivery rate is low. Type II queue is, in fact, optimal from the perspective of minimizing AoI at the destination as the source always ends up transmitting its most recent update arrival. A representative sample path of the AoI process under the Type II queue discipline is presented in Fig. 5. The red upward and blue downward arrow marks indicate the time instants of update arrivals at the source and

deliveries at the destination, respectively. The red plus sign marks indicate the instances of replacing the older update with a newly arrived update and $t_{k,n}$ highlighted in red indicates the n -th replacement of the k -th update.

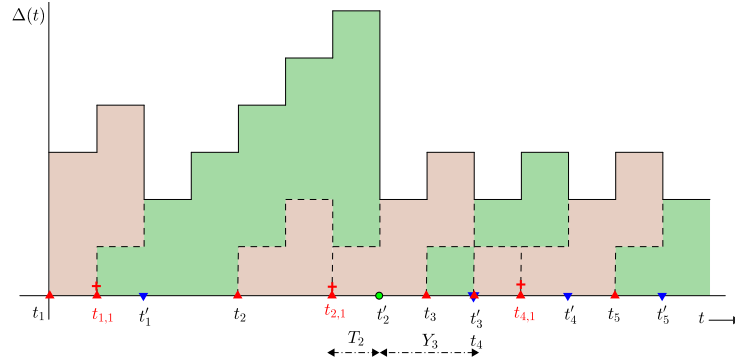


Figure 5. Sample path of the AoI $\Delta(t)$ under the Type II queue discipline.

Similar to the Type I queue analysis presented in Section III, we first present the analysis of the conditional peak AoI for the Type II queue in the following subsection and then characterize its distribution in the subsequent subsection.

A. Conditional Mean Peak AoI

In this subsection, we derive the conditional peak AoI for the typical destination for a given Φ . For this, the primary step is to obtain the means of the inter-departure time Y_k and service time T_k for a given conditional success probability μ_Φ (measured at the typical destination). While it is quite straightforward to determine the mean of Y_k , the derivation of the mean of T_k needs careful consideration of the successive replacement of updates until the next successful transmission occurs.

Mean of Y_k : Recall that the expected time for a new arrival is $\mathbb{E}[S_k] = \mathcal{Z}_a = \frac{1}{\lambda_a} = \frac{1-\lambda_a}{\lambda_a}$. Also, recall that the update delivery rate is $\xi\mu_\Phi$ which follows from the fact that both the successful transmission and the medium access are independent events across transmission slots. Thus, since the transmission starts from the new arrival of the update after the successful departure, the mean time between two departures simply becomes

$$\mathbb{E}[Y_k] = \mathcal{Z}_a + \frac{1}{\xi\mu_\Phi}. \quad (20)$$

Mean and Distribution of T_k : The delivery times T_k restart after every new update arrival before epochs of successful delivery. Let N_k be the number of new update arrivals occurring

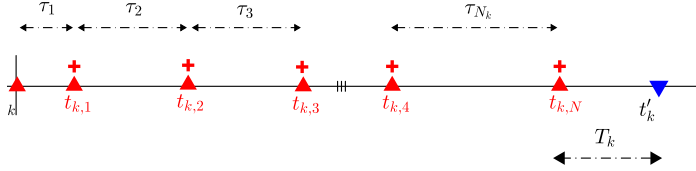


Figure 6. Illustration of the process T_k under Queue Type II.

between the arrival of the k -th update (right after $(k-1)$ -th successful delivery) and the k -th successful transmission, and let τ_n denote the number of slots between the arrivals of two successive updates. Fig. 6 illustrates the typical realization of random process T_k under Type II queue.

The number of slots required to deliver the latest update, i.e. T_k , is given by

$$T_k = S_k - X_{N_k},$$

where $S_k = t'_k - t_k$ and $X_{N_k} = \sum_{i=1}^{N_k} \tau_i$. The number of time slots required for the successful transmission follows geometric distribution with parameter $\xi\mu_\Phi$ and we have

$$\mathbb{P}[S_k = s] = \xi\mu_\Phi(1 - \xi\mu_\Phi)^{s-1}, \quad \text{for } s = 1, 2, \dots$$

Since the arrival process is Bernoulli, inter-arrival times τ_n s between updates are i.i.d. and also follow geometric distribution with parameter λ_a . From the fact that the sum of independent geometric random variables follows negative binomial distribution, we know

$$\mathbb{P}[X_n = K] = \binom{K-1}{n-1} \lambda_a^n (1 - \lambda_a)^{K-n}.$$

Now, we derive the distribution of T_k using the above pmfs of S_k and X_{N_k} . We start by first deriving the probabilities for the boundary values of T_k for given S_k . Since at least one slot is required for the successful update delivery, we have $1 \leq T_k \leq S_k$. From Fig. 6, it can be observed that $T_k = 1$ either if $S_k = 1$ or if there is a new arrival in the S_k -th time slot. Regardless of S_k , therefore, we have

$$\begin{aligned} \mathbb{P}[T_k = 1] &= \mathbb{P}[S_k = 1] + \mathbb{P}[\text{New Arrival Occures in the } S_k \text{-th slot}] \mathbb{P}[S_k > 1] \\ &= \xi\mu_\Phi + \lambda_a(1 - \xi\mu_\Phi). \end{aligned} \tag{21}$$

It is worth noting that $\mathbb{P}[T_k = 1]$ is independent of S_k . The other boundary case, i.e., $T_k = S_k$,

is possible only if there is no new update arrival in $[t_k, t'_k)$. Thus, we have

$$\mathbb{P}[T_k = S_k] = (1 - \lambda_a)^{S_k - 1}. \quad (22)$$

Now, we determine the probability of $T_k = m$ for $m \in \{2, \dots, S_k - 1\}$. For $T_k = m$, the following two conditions must hold so that we get $X_{N_k} = S_k - m$,

- the number of new arrivals within S_k are $N_k \in \{1, \dots, S_k - m\}$, and
- there should not be a new arrival in $[t'_k - m, t'_k]$.

Therefore, for a given $S_k = s$, we have

$$\begin{aligned} \mathbb{P}[T_k = m | S_k = s] &= \mathbb{P}[\text{no arrival in } [t'_k - m, t'_k)] \mathbb{P}[N_k = n \text{ such that } X_n = s - m], \\ &= (1 - \lambda_a)^m \sum_{n=1}^{s+1-m} \mathbb{P}[X_n = s - m], \\ &= (1 - \lambda_a)^m \sum_{n=1}^{s+1-m} \binom{s-m}{n-1} \lambda_a^n (1 - \lambda_a)^{s-m-n}. \end{aligned} \quad (23)$$

Thus, for $S_k = s > 1$, from (21)-(23), we get

$$\mathbb{P}[T_k = m | S_k = s] = \begin{cases} \lambda_a, & \text{for } m = 1, \\ \sum_{n=1}^{s+1-m} \binom{s-m}{n-1} \lambda_a^n (1 - \lambda_a)^{s-n}, & \text{for } m = 2, \dots, s-1, \\ (1 - \lambda_a)^{m-1}, & \text{for } m = s. \end{cases} \quad (24)$$

Finally, we can determine the pmf of T_k for $m > 1$ (i.e. for the last two cases of (24)) as follows

$$\begin{aligned} \mathbb{P}[T_k = m] &= \sum_{s=m}^{\infty} \mathbb{P}[T_k = m | S_k = s] \mathbb{P}[S_k = s], \\ &= \mathbb{P}[T_k = m | S_k = m] \mathbb{P}[S_k = m] + \sum_{s=m+1}^{\infty} \mathbb{P}[T_k = m | S_k = s] \mathbb{P}[S_k = s], \\ &= (1 - \lambda_a)^{m-1} \xi \mu_{\Phi} (1 - \xi \mu_{\Phi})^{m-1} + \underbrace{\sum_{s=m+1}^{\infty} \xi \mu_{\Phi} (1 - \xi \mu_{\Phi})^{s-1} \sum_{n=1}^{s+1-m} \binom{s-m}{n-1} \lambda_a^n (1 - \lambda_a)^{s-n}}_B. \end{aligned} \quad (25)$$

Substituting $s - m = l$ in the term B in (25), we get

$$\begin{aligned} B &= \sum_{l=1}^{\infty} \xi \mu_{\Phi} (1 - \xi \mu_{\Phi})^{l+m-1} \sum_{n=1}^{l+1} \binom{l}{n-1} \lambda_a^n (1 - \lambda_a)^{l+m-n}, \\ &= \xi \mu_{\Phi} (1 - \xi \mu_{\Phi})^m (1 - \lambda_a)^m \sum_{z=2}^{\infty} (1 - \xi \mu_{\Phi})^{z-2} \sum_{n=1}^z \binom{z-1}{n-1} \lambda_a^n (1 - \lambda_a)^{z-1-n}. \end{aligned}$$

Next, by substituting

$$\sum_{n=1}^l \binom{l-1}{n-1} \lambda_a^n (1 - \lambda_a)^{l-n} = \lambda_a,$$

and $z - 2 = a$, we obtain

$$\begin{aligned} B &= \lambda_a \xi \mu_\Phi (1 - \xi \mu_\Phi)^m (1 - \lambda_a)^{m-1} \sum_{a=0}^{\infty} (1 - \xi \mu_\Phi)^a, \\ &= \lambda_a (1 - \xi \mu_\Phi)^m (1 - \lambda_a)^{m-1}, \end{aligned}$$

where the last equality follows using the power series $\sum_{n=0}^{\infty} x^n = \frac{1}{1-x}$ for $|x| < 1$. Finally, substituting B in (25), we get

$$\begin{aligned} \mathbb{P}[T_k = m] &= \xi \mu_\Phi (1 - \xi \mu_\Phi)^{m-1} (1 - \lambda_a)^{m-1} + \lambda_a (1 - \xi \mu_\Phi)^m (1 - \lambda_a)^{m-1}, \\ &= (\xi \mu_\Phi + \lambda_a (1 - \xi \mu_\Phi)) (1 - \xi \mu_\Phi)^{m-1} (1 - \lambda_a)^{m-1}, \end{aligned} \quad (26)$$

for $m > 1$. Therefore, using (21) and (26), we can write

$$\mathbb{P}[T_k = m] = (\xi \mu_\Phi + \lambda_a (1 - \xi \mu_\Phi)) (1 - \xi \mu_\Phi)^{m-1} (1 - \lambda_a)^{m-1}, \text{ for } m = 1, 2, \dots \quad (27)$$

Next, using (27), we derive the mean of T_k as follows:

$$\begin{aligned} \mathbb{E}[T_k] &= (\xi \mu_\Phi + \lambda_a (1 - \xi \mu_\Phi)) \sum_{m=1}^{\infty} m [(1 - \xi \mu_\Phi)(1 - \lambda_a)]^{m-1}, \\ &= \frac{\xi \mu_\Phi + \lambda_a (1 - \xi \mu_\Phi)}{(1 - \xi \mu_\Phi)(1 - \lambda_a)} \sum_{m=1}^{\infty} m [(1 - \xi \mu_\Phi)(1 - \lambda_a)]^m, \\ &\stackrel{(a)}{=} \frac{\xi \mu_\Phi + \lambda_a (1 - \xi \mu_\Phi)}{(1 - [(1 - \xi \mu_\Phi)(1 - \lambda_a)])^2} \\ &= \frac{1}{\xi \mu_\Phi (1 - \lambda_a) + \lambda_a}, \end{aligned} \quad (28)$$

where step (a) follows using the power series $\sum_{m=0}^{\infty} m a^m = \frac{a}{(1-a)^2}$ for $|a| < 1$.

Finally, substituting (20) and (28) in (4), we obtain the conditional mean peak AoI for the Type II queue as

$$\bar{A}_2(\beta; \Phi) = \mathcal{Z}_a + \frac{1}{\xi \mu_\Phi} + \frac{1}{\xi \mu_\Phi (1 - \lambda_a) + \lambda_a}. \quad (29)$$

Remark 2. From (6) and (29), we can verify that

$$\lim_{\lambda_a \rightarrow 1} \bar{A}_1(\beta; \Phi) = \frac{2}{\xi \mu_\Phi} \text{ and } \lim_{\lambda_a \rightarrow 1} \bar{A}_2(\beta; \Phi) = 1 + \frac{1}{\xi \mu_\Phi}.$$

From this, we can say that Type II queue reduces the mean peak AoI almost by a factor of two compared to the Type I queue in the asymptotic regime of λ_a when $\xi \mu_\Phi$ is low.

B. Activity and Distribution of μ_Φ

As the Type II queue just replaces the older updates with the newly arriving updates during the retransmission instances, its transmission rate is the same as that of the Type I queue. In fact, the state diagrams for both these queues are equivalent (please refer to Fig. 3). As a result, the conditional steady state distributions (and thus the conditional activities), for a given μ_Φ , are also the same for both of these queues and are given by (8).

The point process of interferers is characterized by their activities, which is the same for the Type I and II queues. As a result, the distributions of the conditional success probability μ_Φ must also be the same for both of these queues. Based on these arguments, the moments and approximate distribution of the conditional success probability μ_Φ presented in Lemma 1 along with the distribution of transmission activities of interfering sources given in (12) can be directly extended for the analysis of AoI under Type II queue.

C. Moments and Distribution of $\bar{A}_2(\beta; \Phi)$

In this subsection, we derive bounds on the b -th moment and the distribution of the conditional mean peak AoI $\bar{A}_2(\beta; \Phi)$ using the two-step analysis of conditional success probability presented in Section III-D.

Theorem 2. *The upper bound of the b -th moment of the conditional mean peak AoI for Type II queue is*

$$Q_b = \sum_{l+m+n=b} \binom{b}{l, m, n} \mathcal{Z}_a^l \xi^{-m} S(n; m), \quad (30)$$

where

$$S(n; m) = \sum_{k=0}^{\infty} \binom{n+k-1}{k} (1 - \lambda_a)^k \sum_{l=0}^k (-1)^l \binom{k}{l} \xi^l M_{l-m},$$

and M_l is evaluated using Lemma 1 by setting $\bar{p}_m = \bar{p}_m^D$ which is given in (13).

Proof. Let $\mathcal{S}_a = \xi \mu_\Phi (1 - \lambda_a) + \lambda_a$ be the denominator of the last term in (29). Since $\lambda_a \in (0, 1)$, \mathcal{S}_a represents the convex combination of 1 and $\xi \mu_\Phi$. As $\xi \mu_\Phi \in (0, 1)$, we have $0 < \mathcal{S}_a < 1$. Therefore, using the following binomial expansion

$$(1 + x)^{-n} = \sum_{k=0}^{\infty} (-1)^k \binom{n+k-1}{k} x^k \text{ for } |x| < 1,$$

we can write

$$\mathcal{S}_a^{-n} = (1 + (\mathcal{S}_a - 1))^{-n} = \sum_{k=0}^{\infty} (-1)^k \binom{n+k-1}{k} (\mathcal{S}_a - 1)^k.$$

Note that $(\mathcal{S}_a - 1)^k = [\xi\mu_\Phi(1 - \lambda_a) - (1 - \lambda_a)]^k = (-1)^k(1 - \lambda_a)^k(1 - \xi\mu_\Phi)^k$. Using this, we can obtain the expectation of $\mu_\Phi^{-m}\mathcal{S}_a^{-n}$ as

$$\begin{aligned} S(n; m) &= \mathbb{E} [\mu_\Phi^{-m}\mathcal{S}_a^{-n}], \\ &= \mathbb{E} \left[\mu_\Phi^{-m} \sum_{k=0}^{\infty} \binom{n+k-1}{k} (1 - \lambda_a)^k (1 - \xi\mu_\Phi)^k \right], \\ &= \sum_{k=0}^{\infty} \binom{n+k-1}{k} (1 - \lambda_a)^k \sum_{l=0}^k (-1)^l \binom{k}{l} \xi^l M_{l-m}. \end{aligned}$$

Using this and (29), we now derive the b -th moment of $\bar{A}_2(\beta; \Phi)$ as

$$\begin{aligned} Q_b &= \mathbb{E} \left[\left(\mathcal{Z}_a + \frac{1}{\xi\mu_\Phi} + \frac{1}{\xi\mu_\Phi(1 - \lambda_a) + \lambda_a} \right)^b \right], \\ &= \sum_{l+m+n=b} \binom{b}{l, m, n} \mathcal{Z}_a^l \xi^{-m} \mathbb{E} [\mu_\Phi^{-m}\mathcal{S}_a^{-n}]. \end{aligned}$$

Further, substituting $\mathbb{E} [\mu_\Phi^{-m}\mathcal{S}_a^{-n}] = S(n; m)$ in the above expression, we obtain (30). Since the moments of the upper bound of the activity probabilities of interfering sources (given in (13)) are used for evaluating the moments of μ_Φ , the resulting b -th moment of $\bar{A}_2(\beta; \Phi)$ in (30) is in fact an upper bound. \square

The general result presented above can be used to derive simple expressions for the first two moments of $\bar{A}_2(\beta; \Phi)$, which are presented next.

Corollary 3. *The upper bound of the first two moments of the conditional mean peak AoI for Type II queue are*

$$Q_1 = \mathcal{Z}_a + \xi^{-1}M_{-1} + S(1; 0), \quad (31)$$

$$Q_2 = \mathcal{Z}_a^2 + 2\mathcal{Z}_a\xi^{-1}M_{-1} + \xi^{-2}M_{-2} + 2\mathcal{Z}_aS(1; 0) + 2\xi^{-1}S(1; 1) + S(2; 0), \quad (32)$$

where

$$S(n; m) = \sum_{k=0}^{\infty} \binom{n+k-1}{k} (1 - \lambda_a)^k \sum_{l=0}^k (-1)^l \binom{k}{l} \xi^l M_{l-nm},$$

and $M_l = \exp \left(-\pi \lambda_{sd} \beta^\delta R^2 \hat{\delta} C_{\zeta_o}(l) \right)$, such that

$$C_{\zeta_o}(l) = \begin{cases} -\mathbb{E} [\zeta_o (1 - \zeta_o)^{\delta-1}], & \text{for } l = -1, \\ (\delta - 1) \mathbb{E} [\zeta_o (1 - \zeta_o)^{\delta-2}] - (\delta + 1) \mathbb{E} [\zeta_o (1 - \zeta_o)^{\delta-1}], & \text{for } l = -2, \\ \sum_{m=1}^l \binom{l}{m} \binom{\delta-1}{m-1} \bar{p}_m^D, & \text{for } l > 0, \end{cases}$$

and the distribution of ζ_o is given in (12) and \bar{p}_m^D is given in (13).

Proof. Using $\mathbb{E} [\mu_{\Phi}^{-m} \mathcal{S}_a^{-n}] = S(n; m)$ and (29), the mean of $\bar{A}_2(\beta; \Phi)$ can be determined as

$$Q_1 = \mathcal{Z}_a + \xi^{-1} \mathbb{E}_{\Phi} [\mu_{\Phi}^{-1}] + \mathbb{E}_{\Phi} [\mathcal{S}_a^{-1}] = \mathcal{Z}_a + \xi^{-1} M_{-1} + S(1; 0).$$

Similarly, the second moment of $\bar{A}_2(\beta; \Phi)$ can be determined as

$$\begin{aligned} Q_2 &= \mathbb{E} [(\mathcal{Z}_a + (\xi \mu_{\Phi})^{-1} + \mathcal{S}_a^{-1})^2], \\ &= \mathcal{Z}_a^2 + 2\mathcal{Z}_a \xi^{-1} M_{-1} + \xi^{-2} M_{-2} + 2\mathcal{Z}_a S(1; 0) + 2\xi^{-1} S(1; 1) + S(2; 0). \end{aligned}$$

Further, substitution of M_l from Lemma 1 provides the first two moments of $\bar{A}_2(\beta; \mu_{\Phi})$ as in (31) and (32). The values of $C_{\zeta_o}(l)$ for $l \in \{-1, -2\}$ directly follow from Corollary 1. However, the upper limit of the summation in $C_{\zeta_o}(l)$ for $l > 0$ reduces to l (refer to Appendix A). Since the lower bounds of the moments of μ_{Φ} obtained from the two-step analysis are used here, the moments of $\bar{A}_2(\beta; \Phi)$ given in (31) and (32) are the upper bounds (please refer to Section III-D for more details about the constructions and assumptions). \square

The following corollary presents an approximation of distribution of $\bar{A}_2(\beta; \Phi)$.

Corollary 4. *Under the beta approximation, the CDF of the conditional mean peak AoI for Type II queue is*

$$F(x; \beta) = I_{g_{\mu_{\Phi}}(x)}(\kappa_1, \kappa_2) \quad (33)$$

where $g_{\mu_{\Phi}}(x) = \{\mu_{\Phi} \in [0, 1] : \bar{A}_2(\beta; \Phi) = x\}$, and κ_1 and κ_2 are obtain using Lemma 1 by setting $\bar{p}_m = \bar{p}_m^D$.

Proof. Let $g_{\mu_{\Phi}} = \bar{A}_2(\beta; \Phi)$ is a function of μ_{Φ} . Therefore, the CDF of $\bar{A}_2(\beta; \Phi)$ becomes

$$\mathbb{P}[\bar{A}_2(\beta; \Phi) \leq x] = \mathbb{P}[\mu_{\Phi} \leq g_{\mu_{\Phi}}(x)],$$

where $g_{\mu_{\Phi}}(x) = \{\mu_{\Phi} \in [0, 1] : \bar{A}_2(\beta; \Phi) = x\}$. Next, using the beta approximation for the distribution of μ_{Φ} given in Lemma 1, we obtain (33). The parameters κ_1 and κ_2 of the beta

approximation are obtained using the two-step analysis by setting $\bar{p}_m = \bar{p}_m^D$ in (11). \square

V. NUMERICAL RESULTS AND DISCUSSION

This paper presents a new approach of the two-step system level modification for enabling the success probability analysis when the queues at the SD pairs are correlated. Therefore, before presenting the numerical analysis of the peak AoI, we verify the application of this new two-step analytical framework for characterizing the AoI using simulation results in the following subsection. Throughout this section, we consider the system parameter as $\lambda_a = 0.3$ updates/slot, $\lambda_{sd} = 10^{-3}$ links/m², $\xi = 0.5$, $R = 10$ m, $\beta = 3$ dB, and $\alpha = 4$ unless mentioned otherwise.

A. Verification of the Two-Step Analysis

Fig. 7 verifies the proposed analytical framework for different values of R by comparing the simulation results with the analytical results. The curves correspond to the analytical results whereas the markers correspond to the simulation results. This result gives the visual verification of the analysis for $R \in [0, 20]$ which is a wide enough range for the link distance when $\lambda_{sd} = 10^{-3}$ links/m² (for which the dominant interfering source lies at an average distance of around 15 m). Fig. 7 (left) shows that the distribution of the conditional mean peak AoI (obtained using Corollary 2 and Corollary 4 for Type I and Type II queues, respectively) for $R = 20$ is reasonably accurate, which gets even more accurate as the link distance R is decreased. Moreover, the spatial average of the conditional mean peak AoI, i.e., Q_1 , for both the Type I and II queues as shown in Fig. 7 (right) are even more close to the simulation results compared to its distribution given in Fig. 7 (left). This is because an additional approximation (beta approximation) is used to obtain the distribution of $\bar{A}(\beta; \Phi)$.

B. Numerical Results

The performance trends of the conditional mean peak AoI $\bar{A}(\beta; \Phi)$ with respect to the SIR threshold β and the path-loss exponent α are presented in Fig. 8. It may be noted that the success probability decreases with the increase in β and decrease in α . As a result, we can observe from Fig. 8 that the mean of $\bar{A}(\beta; \Phi)$, i.e., Q_1 , also degrades with respect to these parameters in the same order (under both types of queues). As expected, it is also observed that Q_1 increases sharply around the value of β where the success probability approaches to zero. On the other

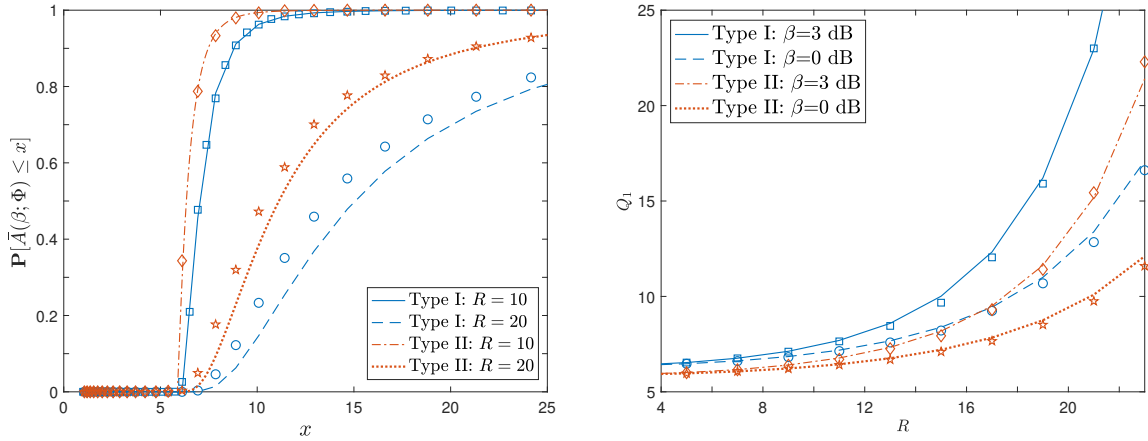


Figure 7. Verification of the proposed analytical framework. The curves correspond to the analytical results whereas the markers correspond to the simulation results.

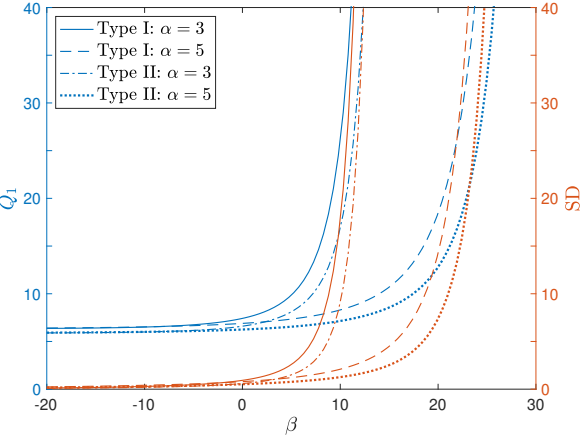


Figure 8. Mean and SD of $\bar{A}(\beta; \Phi)$ with respect to SIR threshold β .

hand, Q_1 converges to a constant value as β approaches to zero where the success probability is almost one. In this region, Q_1 only depends on the packet arrival rate λ_a and medium access probability ξ . For $\lambda_a = 0.3$ and $\xi = 0.5$, we can obtain $Q_1 \approx 6.33$ for Type I queue and $Q_1 \approx 5.56$ for Type II queue by plugging $\mu_\Phi = 1$ in (6) and (29), respectively. These values of Q_1 can be verified from Fig. 8 when $\beta \leq 0$.

Further, it can be observed from Fig. 8 that the standard deviations of $\bar{A}(\beta; \Phi)$ follow a similar trend as that of Q_1 except at $\beta \rightarrow 0$. This implies that the second moment of $\bar{A}(\beta; \Phi)$, i.e., Q_2 , increases at a faster rate than the one of Q_1^2 with respect to β and α . In fact, this trend of Q_1 and Q_2 also holds for the other systems parameters which we discuss next.

Now, we present the performance trends of the mean and standard deviation of the conditional

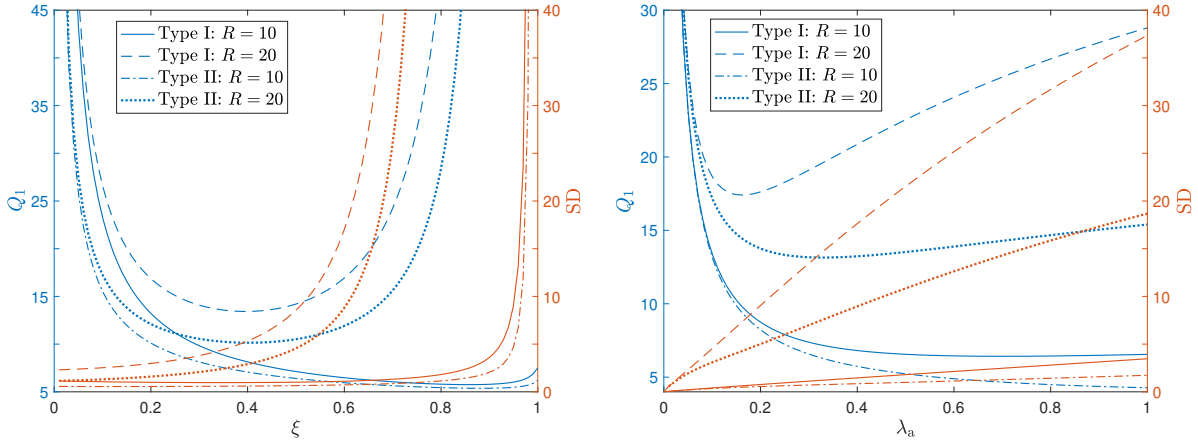


Figure 9. Mean and SD of $\bar{A}(\beta; \Phi)$ with respect to medium access probability ξ , mean peak AoI with respect to the medium access probability ξ and the status update arrival rate λ_a in Fig. 9 (left) and Fig. 9 (right), respectively. From these results, it can be seen that Q_1 approaches to infinity as λ_a and/or ξ drop to zero. This is because the expected inter-arrival times between updates approach infinity as $\lambda_a \rightarrow 0$ and the expected delivery time approaches infinity as $\xi \rightarrow 0$. On the contrary, increasing λ_a and ξ reduces the inter-arrival and delivery times of the status updates which reduces Q_1 . However, Q_1 again increases with further increase in λ_a and ξ . This is because the activities of the interfering SD pairs increase significantly at higher values of λ_a and ξ , which causes severe interference and hence increases Q_1 . However, its rate of increase depends upon the success probability, which further depends upon the wireless link parameters such as the link distance R , SIR threshold β , path-loss exponent α . For example, the figure shows that Q_1 increases at a faster rate with λ_a and ξ when the link distance R is higher.

VI. CONCLUSION

This paper considered a large-scale wireless network consisting of SD pairs whose locations follow a bipolar PPP. The source nodes are supposed to keep the information status at their corresponding destination nodes fresh by sending status updates over time. The AoI metric was used to measure the freshness of information at the destination nodes. For this system setup, we developed a novel stochastic geometry-based approach that allowed us to derive a tight lower bound on the spatial moments of the conditional mean peak AoI under two different queuing disciplines, termed as Type I and II queues. Type I queue is assumed to transmit the status updates in an FCFC fashion with no storage facility. By definition, the new arrivals in this queuing discipline are dropped if the server is busy, which increases AoI at the destination.

To overcome this shortcoming, we consider the Type II queue in which the most recent status update available at the source node in a given transmission slot is transmitted. Type II queue is, in fact, optimal from the perspective of minimizing AoI at the destination as the source always ends up transmitting the most recent update available. That said, the Type I queue analysis is still crucial because it acts as the precursor for the more complicated analysis of the Type II queue.

Our analysis in this paper provided several useful design insights. For instance, our analytical results demonstrated the impact of the update arrival rate as well as the wireless link parameters on the mean and variance of the conditional mean peak AoI. One key observation was that the variance of the conditional mean peak AoI is independent of the arrival rate of the status updates under Type I queue. Another key observation was that Type II queue reduces the mean peak AoI almost by a factor two compared to the Type I queue in the asymptotic regime of the update arrival rate for small values of the successful transmission probability. Our numerical results also revealed that the conditional mean peak AoI can be minimized by appropriately selecting the arrival rate and medium access probability.

REFERENCES

- [1] P. D. Mankar, M. A. Abd-Elmagid, and H. S. Dhillon, “Stochastic geometry-based analysis of the distribution of peak age of information,” 2020, available online: arxiv.org/abs/2006.00290.
- [2] M. A. Abd-Elmagid, N. Pappas, and H. S. Dhillon, “On the role of age of information in the Internet of things,” *IEEE Commun. Magazine*, vol. 57, no. 12, pp. 72–77, 2019.
- [3] S. Kaul, R. Yates, and M. Gruteser, “Real-time status: How often should one update?” in *Proc., IEEE INFOCOM*, 2012.
- [4] R. D. Yates and S. Kaul, “Real-time status updating: Multiple sources,” in *Proc., IEEE Intl. Symposium on Information Theory*, 2012.
- [5] M. Costa, M. Codreanu, and A. Ephremides, “On the age of information in status update systems with packet management,” *IEEE Trans. Inf. Theory*, vol. 62, no. 4, pp. 1897–1910, 2016.
- [6] C. Kam, S. Kompella, and A. Ephremides, “Age of information under random updates,” in *Proc., IEEE Intl. Symposium on Information Theory*, 2013.
- [7] L. Huang and E. Modiano, “Optimizing age-of-information in a multi-class queueing system,” in *Proc., IEEE Intl. Symposium on Information Theory*, 2015.
- [8] K. Chen and L. Huang, “Age-of-information in the presence of error,” in *Proc., IEEE Intl. Symposium on Information Theory*, 2016.
- [9] B. Barakat, S. Keates, I. Wassell, and K. Arshad, “Is the zero-wait policy always optimum for information freshness (peak age) or throughput?” *IEEE Commun. Letters*, vol. 23, no. 6, pp. 987–990, June 2019.

- [10] A. Kosta, N. Pappas, A. Ephremides, and V. Angelakis, "Age and value of information: Non-linear age case," in *Proc., IEEE Intl. Symposium on Information Theory*, 2017.
- [11] A. Javani and Z. Wang, "Age of information in multiple sensing of a single source," 2019, available online: arxiv.org/abs/1902.01975.
- [12] Y. Inoue, H. Masuyama, T. Takine, and T. Tanaka, "A general formula for the stationary distribution of the age of information and its application to single-server queues," *IEEE Trans. Info. Theory*, vol. 65, no. 12, pp. 8305–8324, 2019.
- [13] A. Kosta, N. Pappas, A. Ephremides, and V. Angelakis, "Non-linear age of information in a discrete time queue: Stationary distribution and average performance analysis," 2020, available online: arxiv.org/abs/2002.08798.
- [14] J. P. Champati, H. Al-Zubaidy, and J. Gross, "On the distribution of aoi for the GI/GI/1/1 and GI/GI/1/2* systems: Exact expressions and bounds," in *Proc., IEEE INFOCOM*, 2019.
- [15] O. Ayan, H. M. Grsu, A. Papa, and W. Kellerer, "Probability analysis of age of information in multi-hop networks," *IEEE Netw. Lett.*, 2020.
- [16] R. D. Yates, "The age of information in networks: Moments, distributions, and sampling," 2018, available online: arxiv.org/abs/1806.03487.
- [17] I. Kadota, E. Uysal-Biyikoglu, R. Singh, and E. Modiano, "Minimizing the age of information in broadcast wireless networks," in *Proc., Allerton Conf. on Commun., Control, and Computing*, 2016.
- [18] Y.-P. Hsu, E. Modiano, and L. Duan, "Scheduling algorithms for minimizing age of information in wireless broadcast networks with random arrivals," *IEEE Trans. on Mobile Computing*, to appear.
- [19] M. Bastopcu and S. Ulukus, "Who should google scholar update more often?" in *Proc., IEEE INFOCOM Workshops*, 2020.
- [20] B. Buyukates, A. Soysal, and S. Ulukus, "Age of information in Two-hop multicast networks," in *Proc., IEEE Asilomar*, 2018.
- [21] J. Li, Y. Zhou, and H. Chen, "Age of information for multicast transmission with fixed and random deadlines in IoT systems," *IEEE Internet of Things Journal*, to appear.
- [22] R. Talak, S. Karaman, and E. Modiano, "Minimizing age-of-information in multi-hop wireless networks," in *Proc., Allerton Conf. on Commun., Control, and Computing*, 2017.
- [23] A. Arafa and S. Ulukus, "Timely updates in energy harvesting two-hop networks: Offline and online policies," *IEEE Trans. on Wireless Commun.*, vol. 18, no. 8, pp. 4017–4030, Aug. 2019.
- [24] A. M. Bedewy, Y. Sun, and N. B. Shroff, "Optimizing data freshness, throughput, and delay in multi-server information-update systems," in *Proc., IEEE Intl. Symposium on Information Theory*, 2016.
- [25] Y. Gu, H. Chen, Y. Zhou, Y. Li, and B. Vucetic, "Timely status update in internet of things monitoring systems: An age-energy tradeoff," *IEEE Internet of Things Journal*, vol. 6, no. 3, pp. 5324–5335, 2019.
- [26] M. A. Abd-Elmagid, H. S. Dhillon, and N. Pappas, "A reinforcement learning framework for optimizing age of information in RF-powered communication systems," *IEEE Trans. Commun.*, [Early Access].
- [27] B. Zhou and W. Saad, "Joint status sampling and updating for minimizing age of information in the Internet of Things," *IEEE Trans. Commun.*, vol. 67, no. 11, pp. 7468–7482, 2019.
- [28] M. A. Abd-Elmagid, H. S. Dhillon, and N. Pappas, "Online age-minimal sampling policy for RF-powered IoT networks," *Proc., IEEE Globecom*, Dec. 2019.
- [29] G. Stamatakis, N. Pappas, and A. Traganitis, "Optimal policies for status update generation in an IoT device with heterogeneous traffic," *IEEE Internet of Things Journal*, 2020.

- [30] M. A. Abd-Elmagid, H. S. Dhillon, and N. Pappas, “AoI-optimal joint sampling and updating for wireless powered communication systems,” 2020, available online: arxiv.org/abs/2006.06339.
- [31] B. Buyukates, A. Soysal, and S. Ulukus, “Age of information scaling in large networks,” in *Proc., IEEE ICC*, 2019.
- [32] B. Li, H. Chen, Y. Zhou, and Y. Li, “Age-oriented opportunistic relaying in cooperative status update systems with stochastic arrivals,” 2020, available online: arxiv.org/abs/2001.04084.
- [33] M. A. Abd-Elmagid and H. S. Dhillon, “Average peak age-of-information minimization in UAV-assisted IoT networks,” *IEEE Trans. Veh. Technol.*, vol. 68, no. 2, pp. 2003–2008, Feb. 2019.
- [34] M. A. Abd-Elmagid, A. Ferdowsi, H. S. Dhillon, and W. Saad, “Deep reinforcement learning for minimizing age-of-information in UAV-assisted networks,” *Proc., IEEE Globecom*, Dec. 2019.
- [35] M. K. Abdel-Aziz, C.-F. Liu, S. Samarakoon, M. Bennis, and W. Saad, “Ultra-reliable low-latency vehicular networks: Taming the age of information tail,” in *Proc., IEEE Globecom*, 2018.
- [36] M. Bastopcu and S. Ulukus, “Minimizing age of information with soft updates,” *Journal of Commun. and Networks*, vol. 21, no. 3, pp. 233–243, 2019.
- [37] E. Altman, R. El-Azouzi, D. S. Menasche, and Y. Xu, “Forever young: Aging control for hybrid networks,” in *Proc., IEEE Intl. Symposium on Mobile Ad Hoc Networking and Computing*, 2019.
- [38] E. Hargreaves, D. S. Menasché, and G. Neglia, “How often should I access my online social networks?” in *Proc., IEEE MASCOTS*. IEEE, 2019.
- [39] J. G. Andrews, F. Baccelli, and R. K. Ganti, “A tractable approach to coverage and rate in cellular networks,” *IEEE Trans. on Commun.*, vol. 59, no. 11, pp. 3122–3134, Nov. 2011.
- [40] H. S. Dhillon, R. K. Ganti, F. Baccelli, and J. G. Andrews, “Modeling and analysis of K-tier downlink heterogeneous cellular networks,” *IEEE Journal on Sel. Areas in Commun.*, vol. 30, no. 3, pp. 550 – 560, Apr. 2012.
- [41] F. Baccelli, B. Blaszczyszyn, and P. Muhlethaler, “An aloha protocol for multihop mobile wireless networks,” *IEEE Trans. on Info. Theory*, vol. 52, no. 2, pp. 421–436, Feb 2006.
- [42] Y. Hu, Y. Zhong, and W. Zhang, “Age of information in Poisson networks,” in *Proc., IEEE WCSP*, 2018.
- [43] H. H. Yang, A. Arafa, T. Q. Quek, and V. Poor, “Optimizing information freshness in wireless networks: A stochastic geometry approach,” *IEEE Trans. Mobile Comput.*, [Early Access].
- [44] M. Emara, H. ElSawy, and G. Bauch, “A spatiotemporal model for peak AoI in uplink IoT networks: Time vs event-triggered traffic,” 2019, available online: arxiv.org/abs/1912.07855.
- [45] P. D. Mankar, Z. Chen, M. A. Abd-Elmagid, N. Pappas, and H. S. Dhillon, “Throughput and age of information in a cellular-based IoT network,” 2020, available online: arxiv.org/abs/2005.09547.
- [46] Y. Zhong, T. Q. S. Quek, and X. Ge, “Heterogeneous cellular networks with spatio-temporal traffic: Delay analysis and scheduling,” *IEEE JSAC*, vol. 35, no. 6, pp. 1373–1386, 2017.
- [47] M. Haenggi, “The meta distribution of the SIR in Poisson bipolar and cellular networks,” *IEEE Trans. Wireless Commun.*, vol. 15, no. 4, pp. 2577–2589, 2016.
- [48] M. Haenggi, *Stochastic geometry for wireless networks*. Cambridge University Press, 2012.
- [49] R. R. Rao and A. Ephremides, “On the stability of interacting queues in a multiple-access system,” *IEEE Trans. Inf. Theory*, vol. 34, no. 5, pp. 918–930, Sep. 1988.
- [50] T. Bonald, S. Borst, N. Hegde, and A. Proutiére, *Wireless data performance in multi-cell scenarios*. ACM, 2004.
- [51] Y. Zhong, M. Haenggi, T. Q. S. Quek, and W. Zhang, “On the stability of static Poisson networks under random access,” *IEEE Trans. Commun.*, vol. 64, no. 7, pp. 2985–2998, July 2016.

APPENDIX
PROOF FOR LEMMA 1

The b -th moment of the conditional successful probability μ_Φ given in (2) is

$$M_b = \mathbb{E}_{\Phi, p_{\mathbf{x}}} \left[\prod_{\mathbf{x} \in \Phi} \left(1 - \frac{p_{\mathbf{x}}}{1 + \beta^{-1} R^{-\alpha} \|\mathbf{x}\|^\alpha} \right)^b \right] = \mathbb{E}_\Phi \left[\prod_{\mathbf{x} \in \Phi} \mathbb{E}_{p_{\mathbf{x}}} \left(1 - \frac{p_{\mathbf{x}}}{1 + \beta^{-1} R^{-\alpha} \|\mathbf{x}\|^\alpha} \right)^b \right],$$

where the last equality follows from the assumption of independent activity $p_{\mathbf{x}}$ for $\forall \mathbf{x} \in \Phi$. Now, using the binomial expansion $(1 - x)^b = \sum_{m=0}^{\infty} (-1)^m \binom{b}{m} x^m$ for a general $b \in \mathbb{Z}$, we can write

$$M_b = \mathbb{E}_\Phi \left[\prod_{\mathbf{x} \in \Phi} \sum_{m=0}^b (-1)^m \binom{b}{m} \frac{\bar{p}_m}{(1 + \beta^{-1} R^{-\alpha} \|\mathbf{x}\|^\alpha)^m} \right],$$

where $\bar{p}_m = \mathbb{E}[p_{\mathbf{x}}^m]$ is the m -th moment of the activity. Further, applying the probability generating functional (PGFL) of homogeneous PPP Φ , we obtain

$$\begin{aligned} M_b &= \exp \left(-2\pi \lambda_{\text{sd}} \int_0^\infty \left[1 - \sum_{m=0}^{\infty} (-1)^m \binom{b}{m} \frac{\bar{p}_m}{(1 + \beta^{-1} R^{-\alpha} r^\alpha)^m} \right] r dr \right), \\ &= \exp \left(-2\pi \lambda_{\text{sd}} \sum_{m=1}^{\infty} (-1)^{m+1} \binom{b}{m} \bar{p}_m \int_0^\infty \frac{1}{(1 + \beta^{-1} R^{-\alpha} r^\alpha)^m} r dr \right). \end{aligned} \quad (34)$$

Using [47, Appendix A], the inner integral can be evaluated as

$$\begin{aligned} \int_0^\infty \frac{(\beta R^\alpha)^m}{(\beta R^\alpha + r^\alpha)^m} r dr &= \frac{1}{\alpha} (\beta R^\alpha)^m \int_0^\infty \frac{t^{1-\delta}}{(\beta R^\alpha + t)^m} dt \\ &= (-1)^{m+1} \frac{\beta^\delta R^2}{\alpha} \binom{\delta-1}{m-1} \frac{\pi}{\sin(\delta\pi)}. \end{aligned}$$

Finally, substituting the above solution in (34), we get

$$M_b = \exp \left(-\pi \lambda_{\text{sd}} \beta^\delta R^2 \frac{\delta\pi}{\sin(\delta\pi)} \sum_{m=1}^{\infty} \binom{b}{m} \binom{\delta-1}{m-1} \bar{p}_m \right).$$